

Influence of Elastic and Viscous Effects on Elasto-Viscoplastic Materials

Giovanni M. Furtado^{1,2}, Renato da Rosa Martins¹

¹Department of Mechanical Engineering, Federal University of Rio Grande do Sul, Rua Sarmento Leite 425, Porto Alegre, RS, 90050-170, Brazil

²Federal University of Santa Maria, Rua Ernesto Barros 1345, Cachoeira do Sul, RS, 96506-322, Brazil

Abstract— We use a recently proposed model (de Souza Mendes et al. 2011) for elasto-viscoplastic materials to analyze inertia flows inside a lid-driven cavity. The constitutive equation is a modified version of the viscoelastic Oldroyd-B model in which the viscosity, relaxation and retardation times depend on the material structuring level. The solution is obtained numerically using a three-field Galerkin least-squares-like formulation proposed by Behr et al. 1993, in terms of extra-stress, pressure and velocity. The performance of the constitutive equation and the combined effects of, elasticity and viscoplasticity are analyzed. Results focus on the determination of the yielded and unyielded regions revealing striking effects of these parameters on the flow field.

Keywords—viscoplastic fluid, elasto-viscoplastic model, yield stress, lid-driven cavity, stabilized methods.

I. INTRODUCTION

Elasto-viscoplastic fluids are structured materials that exhibit a complex non-Newtonian behavior that is related to its structure state, which in turn depends on the level of stress applied to it. Below a certain stress threshold, called the yield stress, the material is highly structured, with high levels of elasticity and viscosity. This region can be called the apparent unyielded region. When submitted to stress levels above the yield value, the material experiences a structure break-up leading to a fluid-like behavior where viscosity decays orders of magnitude and elasticity tends to disappear. Recent experiments present some data that show some elastic effects in flows of viscoplastic liquids (de Souza Mendes et al. 2007), Sikorski et al. 2009). This class of materials is present in several important industrial sectors, such as oil, food, pharmaceutical, and cosmetics. The constitutive equation used there was developed as a modified Oldroyd-B equation, which takes into account elasticity below yield stress, and a shear-thinning behavior above yield stress. More recently, a novel and more reliable Oldroyd-B type constitutive equation was proposed de Souza Mendes et al. 2011. One important feature of this equation is that it is also capable to predict the thixotropic behavior of fluids – a characteristic that may be present in many viscoplastic materials.

In this work, we obtain numerical solutions of the governing conservation equations using a three-field Galerkin least-squares-like (GLS) formulation Behr et al. 1993, which takes into account velocity, pressure and extra-stress fields as primal variables. Adding mesh-dependent terms to the governing equations, the formulation is able to successfully capture the elastic and viscous effects present in the used model, even making use of an equal-order combination of linear Lagrangian finite element interpolations. The results focus on the determination of the yielded and unyielded regions revealing striking effects of these parameters on the flow field.

II. MECHANICAL MODELING

The mechanical model for the problem under analysis is made up by the usual mass and momentum governing equations for incompressible fluids, coupled with the constitutive equation for elasto-viscoplastic fluids recently proposed in de Souza Mendes et al. 2011. the conservation equations of mass and momentum, given by:

$$\text{div } \mathbf{u} = 0 \text{ in } \Omega \quad (1)$$

$$\rho (\nabla \mathbf{u}) \mathbf{u} + \nabla p - \text{div } \boldsymbol{\tau} - \mathbf{f} = 0 \text{ in } \Omega \quad (2)$$

1

where \mathbf{u} is velocity vector, $\mathbf{P} = p + \rho \phi$ is the modified pressure, p is the pressure, ρ is the fluid density, and $\mathbf{g} = -\nabla \phi$ is the gravitational force per unit mass.

The constitutive equation of the model adopted in this work for the extra-stress tensor $\boldsymbol{\tau} = \mathbf{T} + \mathbf{p} \mathbf{1}$ is given by:

$$\boldsymbol{\tau} + \theta_1 \overset{\nabla}{\boldsymbol{\tau}} = \eta \left(\overset{\nabla}{\dot{\boldsymbol{\gamma}}} + \theta_2 \boldsymbol{\gamma} \right) \text{ in } \Omega \quad (3)$$

where $\overset{\nabla}{\dot{\boldsymbol{\gamma}}} = \nabla \mathbf{u} + \nabla \mathbf{u}^T$ is the rate of deformation tensor field, and the upper-convected time derivatives of $\boldsymbol{\tau}$ and $\overset{\nabla}{\dot{\boldsymbol{\gamma}}}$ are given by:

$$\overset{\nabla}{\tau} = \frac{d\tau}{dt} - \tau \cdot \nabla \mathbf{u} - \nabla \mathbf{u}^T \cdot \tau \quad (4)$$

$$\overset{\nabla}{\gamma} = \frac{d\dot{\gamma}}{dt} - \dot{\gamma} \cdot \nabla \mathbf{u} - \nabla \mathbf{u}^T \cdot \dot{\gamma} \quad (5)$$

In this model, its rheological parameters, viscosity function (η), relaxation time $\theta_1 = \left(1 - \frac{\eta_\infty}{\eta_{eq}}\right) \frac{\eta_{eq}}{G_{eq}}$ and retardation time $\theta_2 = \left(1 - \frac{\eta_\infty}{\eta_{eq}}\right) \frac{\eta_\infty}{G_{eq}}$ are written in terms of a parameter structure λ , which evolves with the time that the fluid is being submitted to the certain stress. This structure parameter is time dependent, we can just assign it to a thixotropic behavior. In the model used in the present work, the evolution equation for λ is given by:

$$\frac{d\lambda}{dt} = \frac{\partial \lambda}{\partial t} + \mathbf{u} \cdot \nabla (\lambda) = \frac{1}{t_{eq}} \left[(1 - \lambda) - (1 - \lambda_{eq}) \left(\frac{\lambda}{\lambda_{eq}} \right) \right] \quad (6)$$

where the RHS is composed of a (positive) buildup term and a (negative) breakdown term de Souza Mendes et al. 2009.

The parameter t_{eq} is the equilibrium time, which physically means a time scale for the microstructure buildup process. It can be easily observed that when $t_{eq} \rightarrow 0$ the fluid structure instantaneously develops to its equilibrium state and no thixotropic behavior is observed. This situation result in a purely elasto-viscous behavior, and is the situation analyzed in he present work. The relation between the structure parameter and the equilibrium viscosity is given by:

$$\lambda_{eq}(\dot{\gamma}) = \frac{\ln \eta_{eq}(\dot{\gamma}) - \ln \eta_\infty}{\ln \eta_0 - \ln \eta_\infty} \quad (7)$$

where η_0 is the zero-shear-rate viscosity and $\dot{\gamma} = \sqrt{2 \text{tr} \dot{\gamma}^2}$ is

the intensity of $\dot{\gamma}$. The equilibrium structure parameter λ_{eq} is a scalar quantity that varies within the range [0,1]. It gives a measure of the structuring level of the microstructure, i.e., $\lambda_{eq} = 0$ when the structuring level is minimum, and $\lambda_{eq} = 1$ when the material is fully structured.

Therefore, the λ_{eq} can thus be seen as a normalized equilibrium viscosity function, since there is a one-to-one relationship between structure and viscosity levels.

As seen, the relaxation time and retardation time are written in terms of the infinite-shear-rate viscosity η_∞ , the equilibrium viscosity η_{eq} and the equilibrium elastic modulus (de Souza Mendes and Thompson, 2012b), given by:

$$G_{eq} = G_0 e^{m \left(\frac{1}{\lambda_{eq}} - 1 \right)} \quad (8)$$

Where G_0 is the structural elastic modulus of the fully structured material, and m is a positive scalar parameter that dictates the sensitivity of G_{eq} with λ_{eq} . In this equation, it can be observed that its lowest value (i.e., highest relaxation and retardations times) occurs at the highest value of λ , and it increases as λ decays. This function is chosen to simulate the elastic behavior of viscoplastic fluids at the regions of low stress values, i.e., where the stress is below the yield stress.

In this work, we employed the following expression for the equilibrium viscosity (de Souza Mendes and Dutra et al. 2004):

2

$$\eta_{eq}(\dot{\gamma}) = \left[1 - \exp\left(-\frac{\eta_0 \dot{\gamma}}{\tau_y}\right) \left\{ \frac{\tau_y}{\dot{\gamma}} + K \dot{\gamma}^{n-1} \right\} \right] \eta_\infty \quad (9)$$

where η_0 is the low shear rate viscosity plateau, τ_y is the yield stress, K is the consistency index, n the power-law index and η_∞ is the high shear rate viscosity plateau.

2.1 Numerical Approximations

To approximate the mechanical model described above it was employed a multi-field stabilized Galerkin least-squares formulation in terms of velocity, pressure and extra-stress. The classical Galerkin method does not guarantee stable approximations, may generate solutions without physical meaning and numerical pathologies for mixed incompressible fluid flows.

The inherent difficulties associated to the Galerkin method are due to the compatibility of velocity and pressure finite element subspaces, e.g., the need to satisfy the Babuška-Brezzi condition involving these subspaces, a condition which was established by Babuška and Brezzi in the early 70's. The velocity and pressure subspaces may not be spanned by any arbitrary combination of finite element interpolations and, in the case of this work, which employs a multi-field formulation, another compatibility condition must be imposed on the choice of the stress and velocity subspaces. The alternative to remedy Galerkin deficiencies adopted here for incompressible fluid flows was to change the classical Galerkin formulation – adding mesh-dependent terms, which are functions of the residuals of flow governing equations, evaluated element-wise – and use simple Lagrangean elements.

III. NUMERICAL RESULTS

The Fig. 1 schematically shows the $L_c \times L_c$ geometry with the employed boundary conditions: uniform unitary velocity in the x_2 direction on the top wall and non-slip condition ($\mathbf{u}=\mathbf{0}$) at the remaining walls. For all computations, it is used a mesh with 10000 elements, with 10201 nodal points.

A mesh independence procedure evaluating the relative error of the extra-stress magnitude is performed. The Fig. 2 shows a detailed view of the stress profile at $x_1^* = 0.5$. Despite results are almost coincident for the meshes investigated (errors below 3%), the more refined mesh tested – with 100 Q1 finite elements and 10,201 nodal points, which produces a smallest value of its non-dimension element size $h_{K_{min}}^* = h_K/L = 1.41 \cdot 10^{-2}$ is selected in order to guarantee more accurate approximations close the cavity corners.

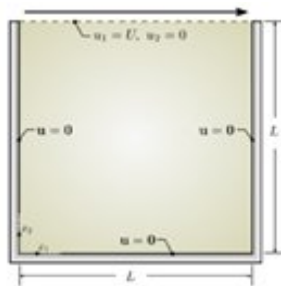


Figure 1 – The geometry

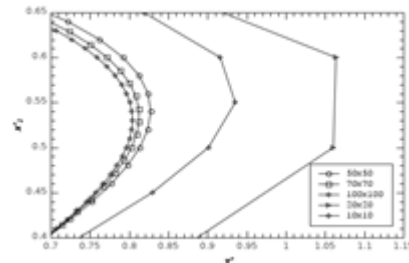


Figure 2 – Mesh independence test

All the simulations are obtained for steady flows, neglecting inertia and thixotropy $t_{eq}^* \rightarrow 0$, i.e., the material structure changes immediately after being submitted to a certain stress level. Also, all the results are obtained for negligible retardation times. The results show the effects of the rheological parameters and of the lid cavity velocity on the yield surfaces. The yield surfaces are defined as the locus of points in which the magnitude of the strain rate is below the lowest shear rate value for which the viscosity equals the higher viscosity plateau where $\eta = \eta_0$, i.e., when, $\dot{\gamma} < \dot{\gamma}_0$ (dos Santos et al., 2011). All the results are obtained for $\eta_\infty^* = 0.01$.

3

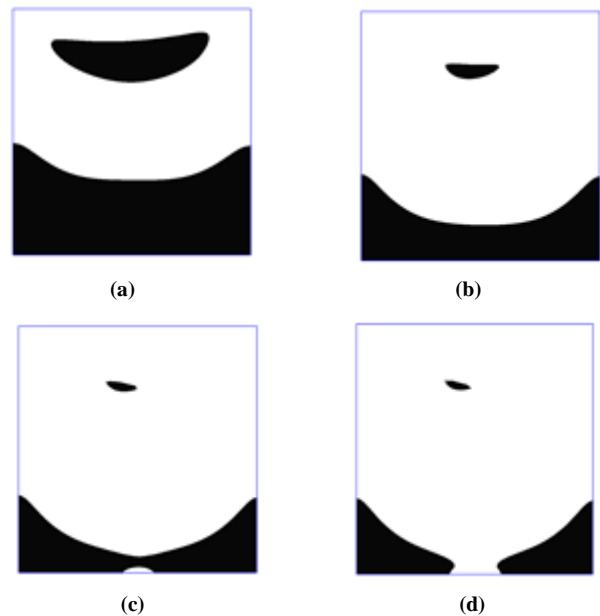


Figure 3 - Yield surfaces: flow intensity influence for $\rho^* = 0$, $\theta_0^* = 100$, $\eta_0^* = 1000$, $\eta_\infty^* = 0,01$ e $m = 20$;
 a) $U^*=0,01$; b) $U^*=0,1$; c) $U^*=0,2$; d) $U^*=0,25$



International Journal of Recent Development in Engineering and Technology
Website: www.ijrdet.com (ISSN 2347-6435(Online) Volume 7, Issue 9, September 2018)

The Fig.(3) show the influence of flow intensity U^* on yield surface topology. As it is noticed, two apparently unyielded regions appear: one close and attached to the bottom wall and another close to the top wall. Both regions decrease as U^* increases throughout the cavity, as expected. The apparently unyielded region close the top wall is associated with the vortex flow, and undergoes a fast decrease as U^* increases, since this region is strongly affected by the increasingly kinematic amounts imposed on cavity lid. The apparently unyielded region at the bottom only experiments a slight decrease, since they are less sensitive to kinematics increase on the cavity lid. In addition, for the highest values of U^* , it is verified that the bottom unyielded region becomes disjointed.

REFERENCES

- [1] Souza Mendes, P.R., and Dutra, E.S.S., 2004, "Viscosity Function for Yield-Stress Liquids", *Applied Rheology*, Vol. 14, pp. 296-302.
- [2] Souza Mendes, P.R., 2007, "Dimensionless non-Newtonian fluid mechanics", *J. Non-Newt. Fluid Mech.*, Vol. 147, pp. 109-116.
- [3] Souza Mendes, P.R., Naccache, M.F., Varges, P.R., Marchesini, F.H., 2007, "Flow of viscoplastic liquids through axisymmetric expansions-contractions", *J. Non-Newt. Fluid Mech.*, Vol. 142, pp. 207-217.
- [4] Behr, M., Franca, L.P., Tezduyar, T.E., 1993. "Stabilized Finite Element Methods for the Velocity-Pressure-stress Formulation of Incompressible Flows", *Comput. Methods Appl. Mech. Engrg.*, vol. 104, pp. 31-48.
- [5] Renato da R. Martins, Giovanni M. Furtado, Daniel D. dos Santos, Sérgio Frey, Mônica F. Nacacche, Paulo R. de Souza Mendes, Elastic and viscous effects on flow pattern of elasto-viscoplastic fluids in a cavity, *Mechanics Research Communications*. 53 (2013) 36-42.
- [6] D. Sikorski, H. Tabuteau, J. R. de Bruyn, Motion and shape of bubbles 452 rising through a yield-stress fluid, *J. Non-Newtonian Fluid Mech.* 159, (2009) 10-16.